

Structural and magnetic phase transition in MnAs(0001)/GaAs(111) epitaxial films

B. Jenichen, V. M. Kaganer, M. Kästner,* C. Herrmann, L. Däweritz, and K. H. Ploog
Paul-Drude-Institut für Festkörperelektronik, Hausvogteiplatz 5–7, D-10117 Berlin, Germany

N. Darowski and I. Zizak
Hahn-Meitner-Institut Berlin GmbH, Glienicke Strasse 100, D-14109 Berlin, Germany

(Received 19 June 2003; published 17 October 2003)

The ferromagnetic phase transition in a MnAs film on GaAs(111), where the MnAs unit cell is epitaxially fixed in its hexagonal plane, proceeds under conditions qualitatively different from the transition in bulk MnAs crystals or in MnAs films on GaAs(001). We present experimental evidence for the coexistence between ferromagnetic and paramagnetic phases in a temperature interval of 10 °C. Temperature dependencies of the phase fractions and the in-plane lattice parameters obtained by grazing incidence x-ray diffraction are compared with magnetization measurements.

DOI: 10.1103/PhysRevB.68.132301

PACS number(s): 68.35.Rh, 64.70.Kb, 61.50.Ks, 75.30.Kz

The combination of magnetic and semiconducting materials leads to new pathways in the development of semiconductor devices utilizing the spin of the carriers.^{1–3} Reliable operation of the devices demands high Curie temperatures of the ferromagnetic materials. A combination of ferromagnetic MnAs and semiconducting GaAs is promising for spin injection devices.⁴ MnAs possesses, at the temperature of approximately 40 °C, a first-order ferromagnetic phase transition. The nature of the transition is discussed since 1960s^{5–9} but still remains controversial.^{10–15} The theories agree that the discontinuous change of magnetization is interrelated with the structural transformation, which involves a lattice-parameter discontinuity as large as 1.2%.^{16,17}

The lattice distortions of the epitaxial films are limited by the epitaxial relationships to the substrate. The MnAs(0001) film on GaAs(111) studied in the present work is epitaxially fixed in the hexagonal plane of MnAs and is free to expand along the c axis of the hexagonal unit cell (Fig. 1). In contrast, the MnAs($\bar{1}\bar{1}00$) film on GaAs(001) is attached by the side facet of the hexagonal unit cell, so that the c -lattice parameter is fixed and the hexagonal plane is orthorhombically distorted in the ferromagnetic α MnAs phase.¹⁸

Recently we have found^{19–22} that the first-order phase transition in MnAs films on GaAs(001) proceeds via a phase coexistence in a large temperature interval. The phase coexistence is caused by the epitaxial constraint on the mean lateral lattice parameter of the film: a discontinuous lattice-parameter variation at the first-order structural transition costs elastic energy and favors the coexistence of elastic domains of the two phases in a large temperature interval. In that former study, the c axis of the hexagonal MnAs unit cell parallel to the GaAs(001) surface resulted in a high degree of in-plane anisotropy of the film: the elastic domains form a striped structure.^{20–23} In contrast, the MnAs layers grown on GaAs(111) are elastically isotropic in the surface plane. As a consequence of the different epitaxial orientations of the MnAs films grown on GaAs(001) and on GaAs(111), differences in the magnetic anisotropies as well as in the strain are observed.^{20–27}

In this paper, we investigate the phase coexistence in a thin MnAs epitaxial layer grown on exactly oriented

GaAs(111)B near the ferromagnetic phase transition α MnAs- β MnAs. Figure 1 shows a schematic view of the epitaxial relationship between GaAs(111) and the hexagonal MnAs lattice. The orthorhombic β MnAs unit cell is also indicated. The unit cell of GaAs can be considered as pseudo-hexagonal.²⁶

The structural change at the α MnAs- β MnAs transition in a bulk crystal consists of a large ($\approx 1.2\%$) lattice-parameter discontinuity in the hexagonal plane and a small ($< 0.2\%$) orthorhombic distortion, while the c -parameter is continuous at the transition.^{17,16} Therefore, we have chosen for the x-ray diffraction study the reflections which lie in the hexagonal plane, α MnAs($\bar{1}100$) and β MnAs(020). These reflections are accessed, for the given film orientation, by the x-ray grazing incidence diffraction technique. The measurements were performed at the bending magnet beamline KMC2 at the storage ring BESSY (Berlin, Germany) using a double crystal graded SiGe(111) monochromator.^{28,29} The energy of the radiation was 8.09 keV. A six-circle x-ray diffractometer with a temperature controlled sample stage was used. The sample temperature was regulated by a standard temperature controller with resistive heating and thermocouple temperature measurement at the sample holder plate. The estimated systematic uncertainty in temperature determination was at most 1 °C. The incidence angle was 0.3°, somewhat larger than the critical angle of the total reflection (0.22°). The angular acceptance of the detector was 0.1°.

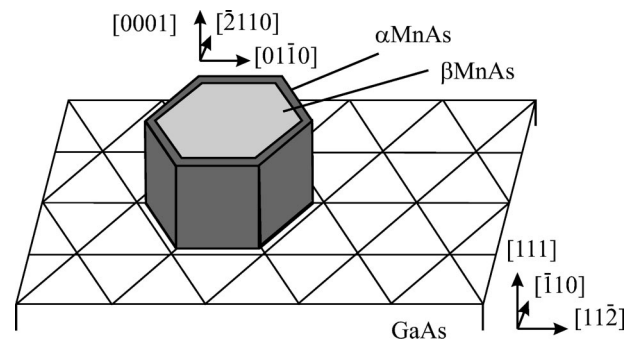


FIG. 1. Schematic view of the epitaxial relationship of MnAs on GaAs(111).

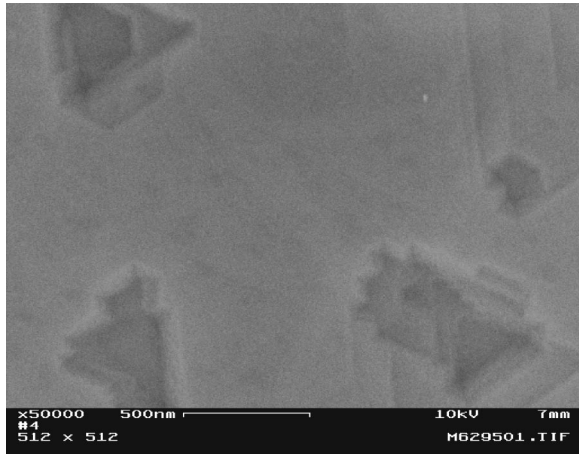


FIG. 2. Scanning electron micrograph of the surface of a 430-nm-thick MnAs film epitaxially grown on GaAs(111)B. A tendency to a threefold symmetry of the growth terraces and the depressions between them is visible. The rms surface roughness on the growth terraces measured by atomic force microscopy is near 10 nm.

The MnAs layers were grown by standard solid source molecular beam epitaxy (MBE), as described elsewhere.²⁶ Commercially available GaAs(111)B epitaxially substrates without intentional miscut were used. The temperature was measured by a thermocouple near the plate of the sample holder. A 100-nm-thick GaAs buffer layer was grown first at 600 °C at a growth rate of 250 nm h⁻¹. Then, a 2-nm-thick MnAs nucleation layer was grown at 225 °C at a growth rate of 20 nm h⁻¹ and an As₄/Mn beam-equivalent pressure (BEP) ratio of 230. The main body of the MnAs layer was grown at 300 °C at a growth rate of 200 nm h⁻¹ and an As₄/Mn BEP ratio of 22. The thickness of the MnAs film is 430 nm as determined by cross-section scanning electron microscopy. Magnetization measurements were carried out using a superconducting quantum interference device magnetometer (Quantum Design Magnetic Property Measurement System) with calibrated temperature stage.

Figure 2 shows a scanning electron micrograph of the surface of MnAs film studied in the present work. The surface exhibits smooth areas and triangularly shaped depressions with a depth of about 100 nm. They originate from the surface morphology of the GaAs buffer, which invariably develops {111} facets during growth on the singular surface in the $\sqrt{19} \times \sqrt{19}$ reconstruction regime.³⁰

Figure 3 presents the temperature variations of the x-ray diffraction curves near the phase transition temperature. A single peak observed below the transition temperature is attributed to the α MnAs($\bar{1}100$) reflection, and the one above the transition temperature to the β MnAs(020) reflection. The β MnAs(020) peak has a higher peak intensity and a larger integrated intensity than the α MnAs($\bar{1}100$) reflection, which is slightly broadened. Near the transition temperature, a continuous transformation from one peak to the other is observed. The peaks are well fitted to sums of two Gaussians, each peak corresponding to one of the two phases. The full widths at half maxima of the Gaussians were fixed at the values obtained from the peaks measured far away from the transition temperature. The peak positions and the integrated

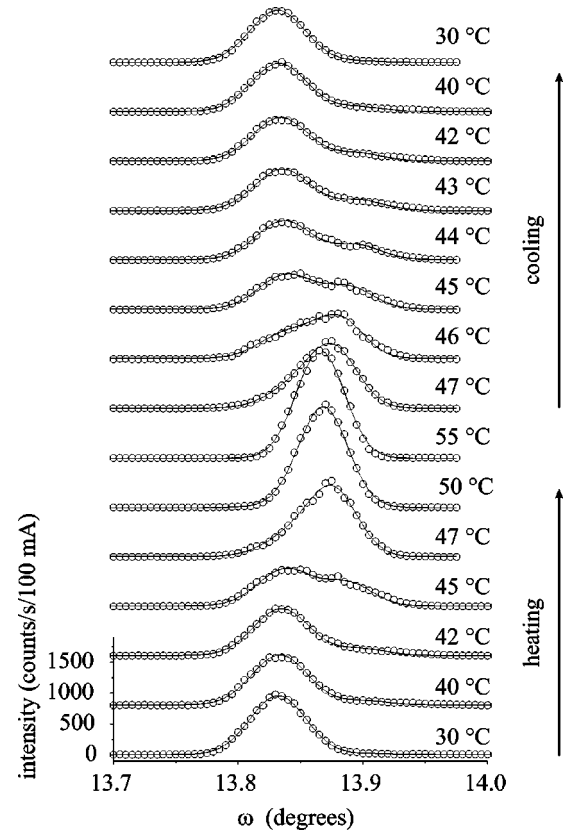


FIG. 3. Grazing incidence diffraction curves ($\omega-2\theta$ scans) near the α MnAs($\bar{1}100$) and the β MnAs(020) reflections measured at different temperatures using grazing incidence synchrotron x-ray diffraction. The circles are the results of the measurements and the lines are the results of the fits to a sum of two Gaussians. The sample temperature is given for each curve.

intensities were fitted. The phase fractions were assumed to be proportional to the integrated intensities scaled by the ones measured in the single phase regions well above and well below the transition temperature.

The temperature dependence of the fraction of the α MnAs phase, calculated from the fits shown in Fig. 3, is presented in Fig. 4(a). Heating and cooling are marked by upward and downward triangles, respectively. The phase coexistence is observed from 40 °C to 50 °C. No temperature hysteresis is seen. The phase coexistence found in the present study for MnAs(0001)/GaAs(111) films occurs at higher temperatures and in a narrower temperature range as compared to the phase coexistence in MnAs($\bar{1}100$)/GaAs(001) films studied in Refs. 19–23, where the phase coexistence with a temperature hysteresis is found in a temperature range 20–40 °C.

Figure 4(b) presents the lattice spacings of both MnAs phases obtained from the peak positions in Fig. 3 and the mean in-plane spacing obtained from the lattice spacings and fractions of the two phases at a given temperature. The mean lattice spacing is expected to be constant in a uniform film. Its variation by plastic deformation is unprobable because of low temperature and reversible variation of the spacings in heating and cooling cycles. However, we find that the mean spacing decreases by approximately 0.24% on heating from

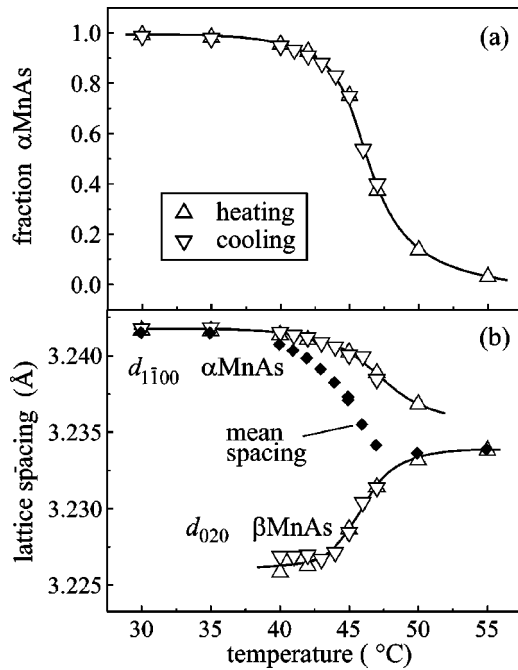


FIG. 4. (a) Temperature dependence of the α MnAs phase fraction near the first-order ferromagnetic-paramagnetic phase transition. Heating and cooling are marked by upward and downward pointing triangles, respectively. (b) Temperature dependencies of the in-plane lattice spacings of the α MnAs and β MnAs phases (empty triangles) and the mean in-plane lattice spacing (full diamonds). The lines are guides for the eye.

the α MnAs to the β MnAs phase. This variation is small compared to the lattice spacing discontinuity in a bulk MnAs crystal at the phase transition¹⁷ of 1.2% and can be explained by the elastic strain relaxation at the surface depressions.

Figure 5 compares the temperature dependencies of magnetization of MnAs films grown on GaAs(111) and GaAs(001). The magnetization of the 430-nm-thick MnAs film on GaAs(111)B (right panel) is nearly isotropic in the plane parallel to the surface. In the absence of an external magnetic field, the magnetization upon heating the sample

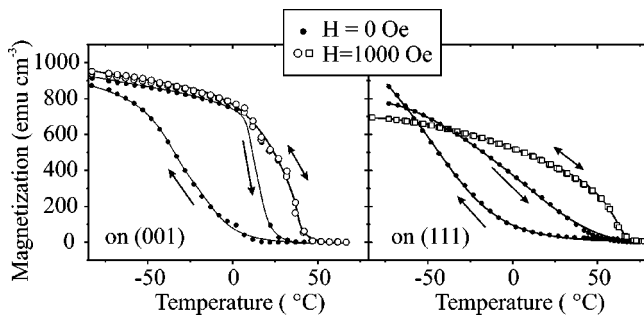


FIG. 5. Temperature dependencies of the magnetization of the 430-nm-thick MnAs epitaxial layer on GaAs(111)B and a 180-nm-thick MnAs epitaxial layer on GaAs(001). Magnetization curves without external magnetic field (full symbols) and in an external magnetic field of 1000 Oe applied along the easy magnetization axis (open symbols) are presented. The rate of the temperature change was $0.5^\circ\text{C}/\text{min}$.

vanishes at approximately 50°C , i.e., at the same temperature where the film completely proceeds into the β MnAs phase, Fig. 4(a). The external magnetic field of 1000 Oe shifts the point where the magnetization vanishes from 50°C to 68°C .

The temperature dependencies of the magnetization of the MnAs films grown on GaAs(001) (left panel in Fig. 5) and GaAs(111) (right panel) in the external field of 1000 Oe consist of two regions: a rapid increase of magnetization in the phase coexistence range and further smooth increase on cooling to $T=0$ K. The rapid increase of magnetization is the result of the increase of the fraction of the ferromagnetic α MnAs phase in the film, Fig. 4(a). For the MnAs film on GaAs(001), the two temperature regions are clearly separated by a kink on the magnetization curve. The magnetization obtained when the whole film transforms into the α MnAs phase is almost 80% of the maximal magnetization reached at $T=0$ K. In contrast, the MnAs film on GaAs(111) reaches just after the phase transition only 25% of the maximal magnetization.

These striking differences in the magnetization of differently oriented films are the result of different epitaxial constraints. In the case of MnAs(1100)/GaAs(001), both the a axis and the c axis of MnAs lie in the interface plane. The phase-transformation strain leads to an orthorhombic distortion of the MnAs unit cell, which still has a freedom to expand normal to the film. However, the distortion does not reduce the magnetization compared to the bulk MnAs crystals.³¹ In MnAs films grown on GaAs(111), the hexagonal plane of MnAs is parallel to the interface. The a lattice parameter is fixed by the epitaxy. The c axis is normal to the surface and the film is free to relax in this direction. From the magnetization change at the transition, which is three times larger for the MnAs film on GaAs(001) compared to the film on GaAs(111), we conclude that the change of the unit cell spacing in the hexagonal plane is necessary to establish the ferromagnetic order.

For binary compounds crystallizing in zincblende and wurtzite structures it is well known that the relative stability of these two structures is closely connected to deviations of the c/a ratio from the ideal value of 1.633, that is, the deviation from the ideal AB_4 tetrahedral coordination polyhedron with four equal bond lengths.^{32,33} Similarly, in compounds crystallizing in the hexagonal NiAs-type structure and the orthorhombic MnP-type structure, the structural transition is characterized by relatively small displacements of atoms.^{16,34} Different types of epitaxy, namely, the epitaxy of the hexagonal MnAs unit cell by a side facet on GaAs(001) or by the hexagonal plane to GaAs(111) change these displacements and considerably influence the magnetic phase transition.

There are further experimental evidences showing that the ferromagnetic phase transition in MnAs is governed by changing the distances between atoms. In MnAs/GaAs(001) films, a small amount of the film is in another orientation, with the c axis in the interface plane along GaAs[110] and the a axis normal to the interface (30° rotated around [0001] with respect to the main orientation). For this additional ori-

entation, a phase transition temperature several degrees higher as compared to that of the main orientation was found.³⁵ The atomic force microscopy shows that the ferromagnetic phase transition temperature in MnAs/GaAs(001) layers is increased in the vicinity of cracks, where the film can relax.³⁶

Thus, the ferromagnetic phase transition in MnAs(0001) epitaxial films on GaAs(111)B proceeds through a phase coexistence of α MnAs and β MnAs, as in the case of MnAs(1100) films on GaAs(001). The phase coexistence is governed by the elastic strain at the discontinuous phase transition with the in-plane lattice expansion limited by the

epitaxy of the film. The transition temperature is notably higher than for MnAs/GaAs(001) films but the magnetization (after the whole film transforms into α MnAs phase) is three times smaller. The strong differences in the ferromagnetic phase transition of differently oriented MnAs epitaxial films are caused by distinct epitaxial constraint of the Mn-As distances and the respective bond angles and can give a new insight into the nature of the magnetic phase transition in MnAs.

The authors thank A. Erko for the beamline support and A. Bluhm for the SEM measurement of the layer morphology.

*Now at European Patent Office, H V Rijswijk, The Netherlands.

¹G.A. Prinz, *Science* **250**, 1092 (1990).

²H. Ohno, *Physica E* **6**, 702 (2000).

³M. Tanaka, *Semicond. Sci. Technol.* **17**, 327 (2002).

⁴M. Ramsteiner, H. Zhu, A. Kawaharazuka, H.-Y. Hao, and K.H. Ploog, *Adv. Solid State Phys.* **42**, 95 (2002).

⁵C.P. Bean and D.S. Rodbell, *Phys. Rev.* **126**, 104 (1962).

⁶R.W. de Blois and D.S. Rodbell, *Phys. Rev.* **130**, 1347 (1963).

⁷K. Bärner, *Phys. Status Solidi B* **88**, 13 (1978).

⁸I.M. Vitebskii, V.I. Kamenev, and D.A. Yablonskii, *Fiz. Tverd. Tela (Leningrad)* **23**, 215 (1981) [*Sov. Phys. Solid State* **23**, 121 (1981)].

⁹I.F. Gribanov and E.A. Zavadskii, *Fiz. Tverd. Tela (Leningrad)* **29**, 949 (1987) [*Sov. Phys. Solid State* **29**, 546 (1987)].

¹⁰P. Ravindran, A. Delin, P. James, B. Johansson, J.M. Wills, R. Ahuja, and O. Eriksson, *Phys. Rev. B* **59**, 15 680 (1999).

¹¹S. Sanvito and N.A. Hill, *Phys. Rev. B* **62**, 15 553 (2000).

¹²A. Continenza, S. Picozzi, W.T. Geng, and A.J. Freeman, *Phys. Rev. B* **64**, 085204 (2001).

¹³Y.-J. Zhao, W.T. Geng, A.J. Freeman, and B. Delley, *Phys. Rev. B* **65**, 113202 (2002).

¹⁴J. Mira, F. Rivadulla, J. Rivas, A. Fondado, T. Guidi, R. Caciuffo, F. Carsughi, P.G. Radaelli, and J.B. Goodenough, *Phys. Rev. Lett.* **90**, 097203 (2003).

¹⁵A.K. Das, C. Pampuch, A. Ney, T. Hesjedal, L. Däweritz, R. Koch, and K.H. Ploog, *Phys. Rev. Lett.* **91**, 087203 (2003).

¹⁶R.H. Wilson and J.S. Kasper, *Acta Crystallogr.* **17**, 95 (1964).

¹⁷B.T.M. Willis and H.P. Rooksby, *Proc. Phys. Soc. London, Sect. B* **67**, 290 (1954).

¹⁸A. Trampert, F. Schippan, L. Däweritz, and K.H. Ploog, *Appl. Phys. Lett.* **78**, 2461 (2001).

¹⁹V.M. Kaganer, B. Jenichen, F. Schippan, W. Braun, L. Däweritz,

and K.H. Ploog, *Phys. Rev. Lett.* **85**, 341 (2000).

²⁰V.M. Kaganer, B. Jenichen, F. Schippan, W. Braun, L. Däweritz, and K.H. Ploog, *Phys. Rev. B* **66**, 045305 (2002).

²¹L. Däweritz, F. Schippan, M. Kästner, B. Jenichen, V.M. Kaganer, K.H. Ploog, B. Dennis, K.-U. Neumann, and K.R.A. Ziebeck, *Inst. Phys. Conf. Ser.* **170**, 269 (2002).

²²B. Jenichen, V.M. Kaganer, F. Schippan, W.B.L. Däweritz, and K.H. Ploog, *Mater. Sci. Eng., B* **B91-B92**, 433 (2002).

²³T. Plake, M. Ramsteiner, V.M. Kaganer, B. Jenichen, M. Kästner, L. Däweritz, and K.H. Ploog, *Appl. Phys. Lett.* **80**, 2523 (2002).

²⁴Y. Morishita, K. Iida, J. Abe, and K. Sato, *Jpn. J. Appl. Phys., Part 2* **36**, L1100 (1997).

²⁵S. Sugahara and M. Tanaka, *J. Appl. Phys.* **89**, 6677 (2001).

²⁶M. Kästner, L. Däweritz, and K.H. Ploog, *Surf. Sci.* **511**, 323 (2002).

²⁷M. Tanaka, K. Saito, and T. Nishinaga, *Appl. Phys. Lett.* **74**, 64 (1999).

²⁸A. Erko, I. Packe, W. Gudat, N. Abrosimov, and A. Firsov, *Nucl. Instrum. Methods Phys. Res. A* **467-468**, 358 (2001).

²⁹A. Erko, N.V. Abrosimov, and V. Alex, *Cryst. Res. Technol.* **37**, 685 (2002).

³⁰K. Yang, J. Schowalter, B.K. Laurich, I.H. Campbell, and D.L. Smith, *J. Vac. Sci. Technol. B* **11**, 779 (1993).

³¹C. Guillaud, *J. Phys. Radium* **12**, 223 (1951).

³²P. Lawaetz, *Phys. Rev. B* **5**, 4039 (1972).

³³L. Däweritz, *Krist. Tech.* **6**, 101 (1971).

³⁴K. Adachi and S. Ogawa, in *Magnetic Properties of Non-Metallic Inorganic Compounds Based on Transition Elements*, edited by H. P. J. Wijn, Landolt-Börnstein, New Series, Group III, Vol. 27a (Springer-Verlag, Berlin, 1988), p. 148.

³⁵F. Iikawa *et al.* (unpublished).

³⁶J. Mohanty, T. Hesjedal, A. Ney, Y. Takagaki, R. Koch, L. Däweritz, and K.H. Ploog, *Appl. Phys. Lett.* **83**, 2829 (2003).